PERGAMON

Deep-Sea Research I 49 (2002) 941–952

DEEP-SEA RESEARCH
PART I

www.elsevier.com/locate/dsr

Instruments and methods

In situ determination of oxygen and nitrogen dynamics in the upper ocean

Steven Emerson[a,*], Charles Stump[a], Bruce Johnson[b], David M. Karl[c]

[a] *School of Oceanography, University of Washington, PO Box 357940, Seattle, WA 98195, USA*
[b] *Department of Oceanography, Dalhousie University, Halifax, NS B3 H 4J1, USA*
[c] *Department of Oceanography, University of Hawaii, Honolulu, HI 96822, USA*

Received 6 June 2001; received in revised form 19 November 2001; accepted 29 November 2001

Abstract

Total gas pressure, oxygen, temperature and salinity were measured at 50 m on a mooring at the Hawaii Ocean Time series (HOT) station from January through September of 1997 and 1998 using a gas tension device (GTD) and a conductivity temperature depth and oxygen (CTD-O_2) sensor (GTD–CTD-O_2 instrument package). Our goal was to evaluate the precision and accuracy of the in situ total gas and oxygen measurements and to assess their utility for remotely determining net biological oxygen production in the euphotic zone. By calibrating the oxygen sensor approximately every month during periodic visits to the mooring it was possible to remotely measure the time history of the partial pressures of nitrogen and oxygen to within $\pm 0.5\%$ accuracy as assessed by independent determination of nitrogen concentration. Oxygen changed at 50 m by 2–4% in a series of episodes with durations of 1–3 months, indicating the discontinuous nature of net O_2 production and the probable decoupling of oxygen production and respiration in the euphotic zone. The GTD and oxygen measurements together can be used to distinguish the effects of physical processes and net biological oxygen production on the oxygen concentrations. The largest uncertainty in the coupled O_2 and total gas pressure measurements is the drift of the oxygen sensor, making frequent calibration presently a necessity. With more complete vertical coverage in the upper ocean it should be possible to use this approach to determine depth-integrated net oxygen production in the euphotic zone and upper thermocline respiration. © 2002 Elsevier Science Ltd. All rights reserved.

Keywords: Gas saturation; Gas-tension device; Deep-sea mooring; Oxygen; Nitrogen; Biological productivity; Subtropical pacific ocean

1. Introduction

Accurate time-series measurements of dissolved oxygen in the surface ocean have proven useful for evaluating the net biological oxygen production if the physical and biological processes causing changes in the oxygen concentration can be separated. Simultaneous measurements of inert gases (Ar, N_2 and He) have been used in models to isolate the biologically induced oxygen changes (Craig and Hayward, 1987, Spitzer and Jenkins, 1989, Emerson et al., 1995). Determination of the net biological oxygen production requires frequent

*Corresponding author. Fax: +1-206-685-3351.
E-mail address: emerson@u.washington.edu (S. Emerson).

0967-0637/02/$ - see front matter © 2002 Elsevier Science Ltd. All rights reserved.
PII: S0967-0637(02)00004-3

measurements over at least one annual cycle and this has been achieved only at ocean time-series sites: near Bermuda in the subtropical Atlantic, near Hawaii in the subtropical Pacific and at Station P in the subarctic Pacific. Because of the labor and expense involved in ship-based time-series studies, oceanographers presently have very few experimentally based estimates of annual net oxygen or carbon production in the euphotic zone of the ocean. If oxygen and inert gas measurements could be made continuously and autonomously, it would be possible to achieve better global coverage of the biological pump with moorings or other remote deployment vehicles.

We present initial results of a method for remotely determining the oxygen and nitrogen gas concentrations using commercially available technology. During the first nine months of 1997 and 1998 nearly continuous total gas pressure, determined by a gas tension device (GTD), and temperature, salinity and oxygen concentrations, from a CTD-O_2 instrument, were measured at the Hawaii Ocean Time series (HOT) station ALOHA. With these data one can determine the partial pressures, concentrations and degrees of saturation of N_2 and O_2. The processes that create changes in gas concentrations in the upper ocean are mixing with deeper waters, gas exchange with the atmosphere (both by diffusive exchange and bubble processes) and the difference between biological production and consumption (Emerson et al., 1995). Heat flux at the surface modifies gas pressures and induces partial pressure disequilibrium. Diffusive gas exchange works to restore the gas concentrations to saturation equilibrium with the atmosphere. Net biological oxygen production, i.e., O_2 production in excess of net community respiration, increases the oxygen concentration without changing the nitrogen concentration. Thus, simultaneous measurement of the two gases can be used to separate the effects of physical and biological processes. (Although nitrogen fixation consumes N_2 in the upper ocean, this process is negligible compared to the effects of bubble processes and gas exchange. For example, Karl et al., 1997, estimate a nitrogen fixation rate of 50–100 $\mathrm{mmol\,N\,m^{-2}\,yr^{-1}}$ at HOT. If we use the higher value and assume it occurs only in the summer, this is equivalent to a N_2 consumption rate of $5\times10^{-4}\,\mathrm{mol\,N\,m^{-2}\,d^{-1}}$. Processes of air injection and gas exchange at the same location, Emerson et al., 1995, drive net fluxes of N_2 between the atmosphere and ocean at HOT of $100\text{–}200\times10^{-4}\,\mathrm{mol\,N_2\,m^{-2}\,d^{-1}}$. Thus, even the maximum N_2 uptake by nitrogen fixation is $\leqslant5$ percent of the physically induced fluxes at this site.

We compare the in situ data with frequent, independent measurements of oxygen and nitrogen gases. Our goal is to evaluate the performance of the instruments and the efficacy of this approach. Since our data are from a single depth, we do not have sufficient information to determine, with any accuracy, the annual integrated net biological oxygen production in the euphotic zone, but we can qualitatively evaluate the importance of intermittent physical and biological events in determining the oxygen mass balance.

2. Methods and setting

2.1. Analytical

The measurement system consists of a GTD attached to a CTD-O_2 sensor package. The GTD (Anderson and Johnson, 1992; McNeil et al., 1995; Pro-Oceanus Systems Inc., Brookside, NS, Canada) determines total gas pressure in water using a Paroscientific pressure sensor. The sensor is in contact with gases dissolved in the water via a small tube sealed with a silastic membrane supported on a rigid template so that the measurement is insensitive to hydrostatic pressure. The capability of this instrument for determining total gas pressure in upper ocean waters has been demonstrated (McNeil et al., 1995, Farmer et al., 1993), but the data have never before been compared to independent nitrogen gas measurements. The CTD-O_2 instrument is a SEACAT CTD with a YSI pulsed oxygen electrode, both purchased from the Seabird Company, Bellevue, WA, USA.

The instrument was deployed at 50 m on a mooring (23.27°N and 158.08°W) 30 km south of the HOT Station. This depth was chosen because it is within the shallow O_2 maximum at this location.

The mooring, HALE-ALOHA (Letelier et al., 2000; http://hahana.soest.hawaii.edu), began operation in January 1997. We present data from four roughly 6-month deployments (HALE 1–4, 11 January 1997–12 May 1997; 19 May 1997–1 December 1997; 19 December 1997–18 April 1998; 28 May 1998–7 November 1998). The instrument records hydrostatic pressure, T, S, gas tension, and oxygen concentration every 2 h during these periods. Between deployments the O_2 sensor membrane and filling solution were changed, and the entire package was cleaned and refitted with poisons to delay biological fouling.

Independent measurements of oxygen were determined from hydrocasts near the mooring site on the deployment and recovery cruises and at roughly monthly intervals in between. Nitrogen gas measurements were also made on many of the cruises (Table 1). Oxygen was determined by Carpenter Winkler titations and N_2/O_2 and Ar/O_2 ratios were determined on separate water samples by mass spectrometry (Emerson et al., 1995). Accuracies of both methods are described in Emerson et al. (1999).

2.2. Calculation of N_2 and O_2 pressures and concentrations

The total gas pressure of the atmosphere, P^a, is equal to the sum of the partial pressures, p_i^a, of all the atmospheric gases. The units are atmospheres (atm) or millibars (mbar), where 1 atm pressure $= 1013.25$ mbar. If we neglect those partial pressures below 20 μatm the total atmospheric

Table 1
T, S, $[O_2]$, and $[N_2]$ measurements made at 50 m during deployment and recovery of the mooring and during approximately monthly cruises to his site

Deployment	Julian day	T (°C)	S (ppt)	$[O_2]$ (μmol/kg)	Corr (%)	$[N_2]$ (μmol/kg)	$N_{2,ss}$ (%)
HALE 1	12,1997	23.895	34.899	210.6	—	395.5	0.3
	50	23.845	34.929	212.3	−0.0		
	72	22.860	35.031	217.9	0.4	409.2	1.3
	102	23.310	34.974	216.2	1.1		
	128	24.441	34.883	215.4	6.7	397.9	2.0
HALE 2	141	24.569	34.895	214.0	—	397.9	2.0
	157	24.756	34.933	211.3	1.5		
	214	25.185	35.120	215.1	1.0	396.4	2.6
	268	26.542	35.176	209.1	17.4	388.7	0.4
	318	25.670	35.135	213.1	13.8	395.5	0.8
HALE 3	353	23.713	35.146	211.7	—	400.4	1.5
	13,1998	22.720	35.256	215.7	3.6		
	50	22.787	35.239	215.9	−1.1		
	52	22.787	35.239	216.9	0.2		
	107	23.699	35.203	214.0	5.7		
HALE 4	118	23.789	35.209	212.1	—	400.2	1.7
	134	23.527	35.220	213.8	0.6		
	168	24.055	35.255	215.1	1.7		
	197	24.428	35.337	213.3	7.1		
	223	24.273	35.440	217.7	10.1		
	272	26.084	35.351	202.5	11.6		
	293	25.226	35.438	208.1	4.3		

$[O_2]$ was used to calibrate the oxygen sensor. The O_2 sensor correction in percent (%) is indicated in the "Corr" column. N_2 concentration and supersaturation, $N_{2,ss}$, determinations using the methods outlined in Emerson et al. (1999) are compared with the GTD–CTD-O_2 estimates of these values in Fig. 8.

pressure is

$$P^{a} = p^{a}_{N_2} + p^{a}_{O_2} + p^{a}_{Ar} + p^{a}_{H_2O} + p^{a}_{CO_2}. \quad (1)$$

The mole fraction of each gas, i, in the atmosphere, X_i is its fraction in dry air ($\text{moles}_{\text{gas}}\,\text{mole}^{-1}_{\text{air}}$, $l_{\text{gas}}\ l^{-1}_{\text{air}}$, ppmv, etc.) and is thus related to its partial pressure in the atmosphere, p^{a}_{i}, via the total pressure and the partial pressure of water vapor, $p^{a}_{H_2O}$.

$$X_i = p^{a}_{i}/(P^{a} - p^{a}_{H_2O}). \quad (2)$$

In dry air, when $p^{a}_{H_2O} = 0$, the ratio of the partial pressure to total pressure and mole fraction are equal. We use the values of Glueckauf (1951) for X_{N_2}, X_{O_2} and X_{Ar} (0.78084, 0.20946 and 0.00934, respectively), and X_{CO_2} is presently 0.000365.

The quantity measured by the GTD is the total gas pressure in water, and is, similarly equal to the partial pressures of each of the gases in water, p^{w}_{i}:

$$P^{w} = p^{w}_{N_2} + p^{w}_{O_2} + p^{w}_{Ar} + p^{w}_{H_2O} + p^{w}_{CO_2}. \quad (3)$$

In order to interpret the GTD results in terms of oxygen and nitrogen pressure we assume that the other three gases are at equilibrium with the atmosphere; that is, $p^{w}_{i} = p^{a}_{i}$ for CO_2, Ar and H_2O. We argue that these assumptions introduce errors that are less than the accuracy of our measurements (± 0.1–0.2%). The partial pressure of CO_2 in the ocean is rarely at equilibrium with the atmosphere, and seasonal changes can be as large as several hundred ppm in some locations (Takahashi et al., 1997). This large variability, however, represents changes of only ± 0.01 percent of P^{W}, so it is reasonable to assume saturation equilibrium for CO_2. Many argon measurements in the ocean (Emerson et al., 1995; Spitzer and Jenkins, 1989) indicate that it is several percent undersaturated in the deep ocean and rarely more than ten percent supersaturated in surface waters. The maximum error of assuming saturation is thus $< \pm 10\%$ of roughly one percent or $\pm 0.1\%$. Water vapor is saturated in the air immediately above the ocean surface; thus, if the atmospheric pressure is determined near the surface on a buoy, it includes equilibrium vapor pressure of water. The atmosphere inside the pressure chamber of the GTD should also be saturated with water because the instrument is submerged and the silastic membrane is highly permeable to H_2O vapor (Brandrup et al., 1999). As the saturation pressure in seawater at 25°C is about 3%, the equilibrium assumption must be accurate to better than $\pm 3\%$ to achieve an accuracy of $\pm 0.1\%$ for the determination of total gas pressure of N_2 as O_2. Clearly, the last assumption, namely that water vapor pressure inside the GTD is at equilibrium with the surroundings, contains the most probable cause of inaccuracy. Because the response time of the GTD is on the order of hours (B. Johnson, unpublished results), the pressure chamber should be saturated with water vapor at the ambient seawater temperature in the absence of large and rapid temperature changes in the upper ocean. If these assumptions are valid (they are tested later in Section 5 (Conclusions)), the difference in pressure between the GTD and atmospheric pressure determinations equals the excess nitrogen plus oxygen gas pressure in the water:

$$(p^{w}_{N_2} - p^{a}_{N_2}) + (p^{w}_{O_2} - p^{a}_{O_2}) = P^{w} - P^{a}. \quad (4)$$

To separate the partial pressures of nitrogen and oxygen we calculate the oxygen pressure from measured oxygen concentrations and published solubility determinations. The fugacity, f^{w}, of a gas in the water is related to its concentration per unit mass of seawater, [C] ($\text{mol}\,\text{kg}^{-1}$) via the solubility coefficient, $S_{H,C}$ ($\text{mol}\,\text{kg}^{-1}\,\text{atm}^{-1}$), which is a function of temperature and salinity. The solubility coefficient is equivalent to the Henry's Law coefficient, $K_{H,C}$, except that it has units of $\text{mol}\,\text{kg}^{-1}\,\text{atm}^{-1}$ rather than $\text{mol}\,\text{l}^{-1}\,\text{atm}^{-1}$.

$$f^{w}_{C}\{S_{H,C}\} = [C]. \quad (5a)$$

Since N_2, O_2, and Ar behave nearly ideally in the atmosphere (Benson and Krause, 1984), we assume that fugacities and partial pressures are equal ($f^{w} = p^{w}$) and therefore,

$$p^{w}_{C}\{S_{H,C}\} = [C]. \quad (5b)$$

The partial pressure in the water can be thought of as the gas pressure that would be in equilibrium with the seawater concentration at the measured temperature and salinity. At saturation equilibrium the partial pressures of a gas in the atmosphere and water are the same and equal to

the values in a water-vapor saturated atmosphere (see Benson and Krause, 1984). Eq. (5b) is the general relationship between gas concentration and partial pressure in the water, and it can be combined with Eq. (2) to derive the relationships among atmospheric mole fraction, total atmospheric pressure, equilibrium water-vapor pressure and the saturation concentration. At saturation equilibrium (indicated by the superscript s):

$$X_C(P^a - p^s_{H_2O})S_{H,C} = [C^s]. \quad (6)$$

The partial pressure of nitrogen in the water can now be written in terms of the known and measured quantities using Eqs. (2), (3) and (5b).

$$\begin{aligned} p^w_{N_2} &= P^w - \{P^a - p^s_{H_2O}\}(X_{Ar} + X_{CO_2}) \\ &\quad - p^s_{H_2O} - [O_2]/S_{H,O_2} \\ &= P^w - P^a(X_{Ar} + X_{CO_2}) \\ &\quad + p^s_{H_2O}(X_{Ar} + X_{CO_2} - 1) - [O_2]/S_{H,O_2} \\ &= P^w - 0.00970\,P^a + 0.99030\,p^s_{H_2O} \\ &\quad - [O_2]/S_{H,O_2}. \end{aligned} \quad (7)$$

We use the equations presented in Garcia and Gordon (1992) for the solubility coefficient for

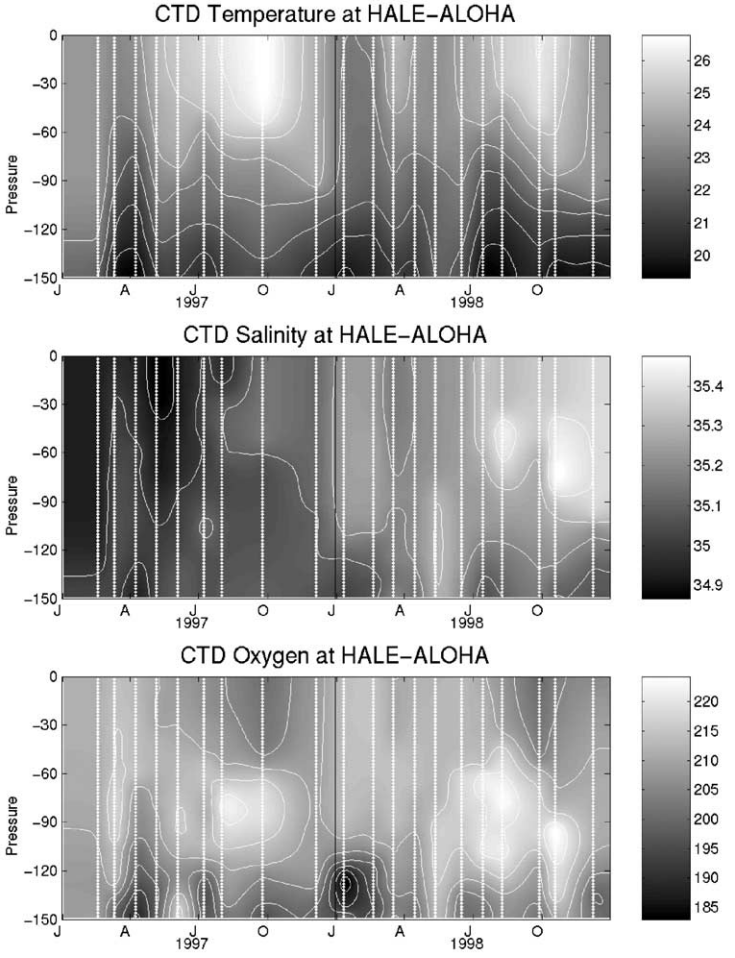


Fig. 1. Contours of temperature, salinity and oxygen vs. depth and time from roughly monthly profiles for the period 1997 and 1998 at the HALE-ALOHA mooring of HOT. The GTD–CTD-O_2 instrument was deployed at 50 m. Data are from the HOT web site http:\\\hahana.soest.hawaii.edu.

oxygen in seawater as a function of temperature and salinity.

Determination of P^w, $[O_2]$, T, and S in the water and P^a in the atmosphere provides all the information necessary to compute the pressure and concentration of nitrogen (Eqs. (7) and (5b)). The departures of nitrogen and oxygen from atmospheric saturation are determined from Eqs. (5b) and (6). For the nitrogen saturation value we use the correction to the compilation of Weiss (1970) suggested by Emerson et al. (1999). GTD and atmospheric pressure measurements are highly accurate ($\pm 0.01\%$ claimed by the manufacturer, Paroscientific Instruments), and atmospheric saturation values are known for these gases to within $\pm 0.2\%$. The greatest uncertainty in the calculations is the measurement of the oxygen concentration. It is well known that oxygen sensors drift with time (months), and our measurements are no exception. Because we are working at one of the ocean time-series stations we were able to calibrate the oxygen sensor roughly once per month during the course of the experiment.

3. Results

Contour plots of T, S and O_2 in the upper 150 m of the ocean at Station ALOHA for the years 1997 and 1998 (Fig. 1, data available at the HOT web site, http://hahana.soest.hawaii.edu) provide the oceanographic background to aid interpretation of the in situ data. One can see that as the thermocline develops the seasonal mixed layer passes from below to above the depth of 50 m, and in summer is just above the subsurface oxygen maximum created by net photosynthesis and warming. We also made independent measurements of oxygen and nitrogen gas concentrations at the mooring site, HALE ALOHA, during many of the recovery and deployment cruises. These data and some from the near-by HOT time-series location are presented in Table 1 and used later to compare to the in situ instrument measurements of oxygen and nitrogen saturation. Atmospheric pressure data were taken from NODC buoy number 51001 in the vicinity (23°24.04′N, 162°15.59′W).

Changes with time in temperature, salinity, total gas pressure and oxygen concentration at 50 m at the mooring location are presented in Figs. 2–4. The temperature data (Fig. 2a) indicate warming in which the temperature at this depth increased by about 3° in 1997 and 1° in 1998 during the first 9 months of the year. The warming is not smooth but is punctuated with rapid excursions and exhibits "noise". Much of the short-term (daily) variation is a result of the excursion of the sensor package 2–4 m daily due to internal tides, inertial period oscillations and wire motion (determined from hydrostatic pressure measurements, not shown). For example, the moored sensor effectively moves up and down in the gradients of temperature and salinity. Other changes in both the temperature and salinity (Fig. 2) on time scales of months are caused by passing of fronts and eddies. The very rapid cooling and salinity increase that occurred in early March and lasted until mid April in 1997 is the result of a mesoscale eddy that entered the area. This feature was associated with

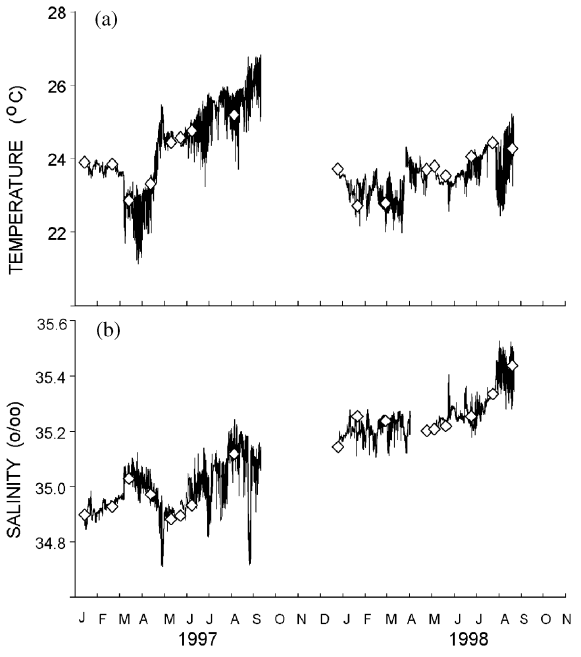


Fig. 2. Temperature (a) and salinity (b) determined every 2 h at 50 m by the GTD–CTD-O_2 instrument (lines) during HALE 1–4 deployments for the years 1997 and 1998. Diamonds are data from independent CTD casts near the mooring.

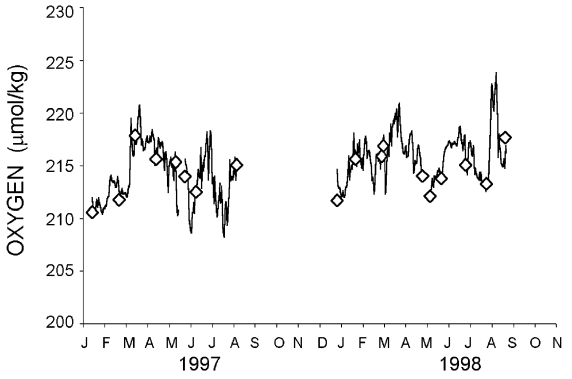


Fig. 3. Daily averaged oxygen concentrations determined from measurements every 2 h at 50 m by the GTD–CTD-O_2 instrument (lines) during HALE 1–4 deployments for the years 1997 and 1998. Diamonds are oxygen measurements from the same density as the instrument determined by Winkler titrations. The O_2 sensor is calibrated to the Winkler titrations to correct for instrument drift (see Table 1).

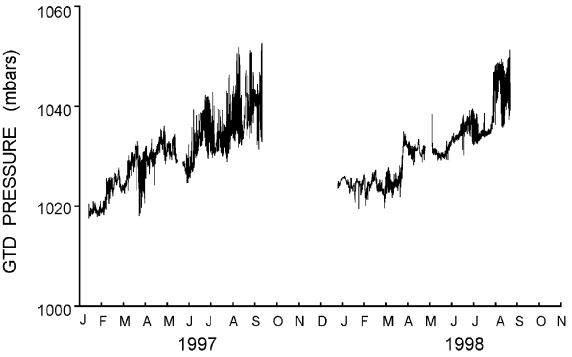


Fig. 4. Total gas pressure determined from measurements every 2 h at 50 m by the GTD–CTD-O_2 instrument during HALE 1–4 deployments for the years 1997 and 1998.

dramatic change in sea surface height, shoaling of the thermocline, local upwelling calculated from wind divergence measurements, high chlorophyll (Letelier et al., 2000) and oxygen and nitrogen gas changes (see later).

The oxygen concentration data from the mooring (Fig. 3) are presented as daily averages to smooth some of the noise caused by movement of the sensor with respect to depth. Inspection of the data before averaging revealed little diurnal variation consistent with light and dark cycles. The data diamonds in Fig. 3 are not, in this case, independent of the curve. The sensor output was calibrated to these data assuming that the drift was linear between calibration times. The extent of sensor drift is indicated by the amount of adjustment required at each calibration (Table 1). The sensitivity of the oxygen sensors deteriorates with time, probably because of biological fouling and slow changes in concentration of the electrolyte filling solution. We judged that the assumption of linear drift between calibrations became unreliable after the correction exceeded 10%, and we do not interpret any oxygen sensor result that required a greater correction (i.e., the last 104 days of HALE 2 and 70 days of HALE 4, Table 1).

One clear feature in the oxygen data is variability that is missed by the monthly ship-based sampling. There are "episodes" of oxygen increase by 2–5% followed by a decrease of the same magnitude with a cycle of 1–3 months. The 1997 data have two of these episodes and the 1998 data, four. The details of these changes could not have been determined without the sensor measurements. Other than this remarkable variability, there is no discernible annual trend in oxygen concentration data. A linear regression through the results is a horizontal line with a standard deviation of $\pm 2.5\%$ ($215 \pm 5\,\mu mol/kg$).

Results from the measurement of total gas pressure (Fig. 4) indicate a gradual increase through the year with daily and monthly cycles superimposed. There was no correlation between the short-term (daily) GTD and hydrostatic pressure measurements (data not shown), indicating the rigid template effectively supports the GTD membrane removing any effect of hydrostatic pressure change. Longer changes with time exhibit an episodic character with periods of between one and three months. A linear regression through the data indicates there is a clear trend of increasing pressure. (The slope and fit of the linear regressions are $m = 0.082$, $r^2 = 0.75$ and $m = 0.081$, $r^2 = 0.78$ for the data of 1997 and 1998, respectively). Over the first 9 months of the year this represents a 20 mbar, or approximately 2%, increase with a scatter of $< \pm 0.5\%$.

Total gas pressure from the GTD is plotted along with atmospheric pressure from the weather buoy in the vicinity in Fig. 5. The total gas pressure in the ocean increases through the year

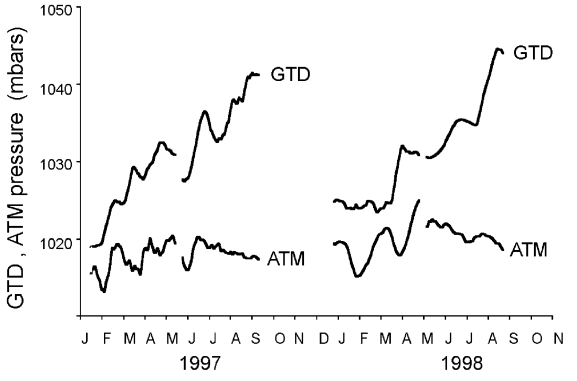


Fig. 5. Total gas pressure from the GTD data (upper line) and atmospheric pressure from a near-by NODC buoy (lower line) during the period 1997 and 1998. Both lines are two-week running means through the raw data.

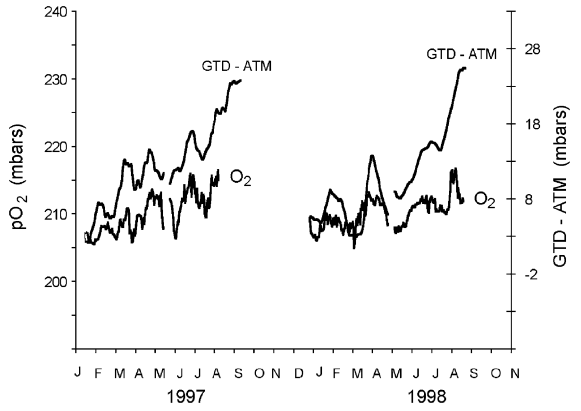


Fig. 6. The daily mean difference between the total gas pressure and the atmospheric pressure (GTD−ATM) as a function of time (upper line), and the oxygen partial pressure, pO_2 (lower line), calculated from the oxygen concentration, temperature, and salinity data and the oxygen solubility.

while the atmospheric pressure indicates no clear trend. Both sets of data are smoothed with a two-week running mean to filter the short-term noise due to movement of the sensor in the vertical gradient. Comparison between Figs. 4 and 5 demonstrates that this procedure does not distort the general trends GTD results. The atmospheric mean includes data two weeks prior to the date indicated, whereas the GTD two-week mean is centered on the reported date. This corrects for the lag in response time of gases in the upper ocean, which have a residence time with respect to gas exchange of weeks. Various lag periods of between 1 and 4 weeks created very little change in the GTD−atmospheric difference (data not shown). The total gas pressures in the ocean at 50 m and in the atmosphere are within 5 mbar of each other in January. Previous measurements of both N_2 and Ar at this location (Emerson et al., 1997) indicate low levels of supersaturation in winter caused by a combination of surface water cooling and bubble processes.

The increase in the GTD−atmospheric pressure difference (GTD−ATM, Fig. 6) is caused by a combination of water temperature changes and the changes in the concentrations of N_2 and O_2 due to gas exchange, bubble processes and net biological production (for O_2). The results in Fig. 6 indicate that the ''episodes'' of oxygen concentration increase and decrease are clearly visible in the GTD data. The results in this figure also indicate that the (GTD−ATM) pressure change is not solely the result of oxygen pressure changes. The two measurements diverge with time in both 1997 and 1998, indicating that part of the pressure change in the water is caused by nitrogen gas.

4. Discussion

Gas pressure and concentration in the upper ocean are influenced by processes within the ocean and exchange with the atmosphere. Nitrogen concentrations in the upper 500 m in the subtropical ocean are 1–2 % supersaturated (Emerson et al., 1995) because this was the concentration of the gas in the water when it left the ocean's surface. Since the temperature decreases with depth below the mixed layer, the concentration of nitrogen gas [N_2] increases. Upwelling or mixing of surface waters with deeper waters thus does not create an appreciable change in N_2 pressure or the degree of saturation (with the exception of that caused by a slight nonlinearity in the gas saturation—temperature relationship), but does change the N_2 concentration. Warming of the surface ocean in a system closed to the atmosphere has no effect on the gas concentration, but increases the gas

pressure through the Henry's Law relationship (Eq. (5a)). Exchange with the atmosphere resulting from surface-ocean disequilibrium or from bubble dissolution in the water caused by breaking waves affects both the concentration and pressure of N_2 and O_2. Both the pressure and concentration of oxygen are also altered by net community biological production in the euphotic zone, and net community respiration below the euphotic zone.

Temperature change and bubble processes are the primary reasons for the gradual increase in the gas pressure (GTD−ATM) in Fig. 6. We can eliminate the effect of temperature on the temporal evolution of the nitrogen by calculating the nitrogen concentration via Eqs. (7) and (5b) (Fig. 7). There is a dramatic increase in nitrogen concentration in March 1997. As described earlier, this change is the result of a cyclonic eddy that entered the area. Divergence of winds in the region caused a localized upwelling at the same time as the eddy-induced shoaling of the isopycnals (Letelier et al., 2000). The change in both temperature (Fig. 2a) and nitrogen gas indicate values at 50 m that are normally at about 125 m at this location. The increase in nitrogen gas results from lifting of the isopycnals by as much as 75 m as the eddy passed through the area. The gradual decrease in nitrogen concentration during the remainder of the year (Fig. 7) resulted from passing of the eddy from the area and export of

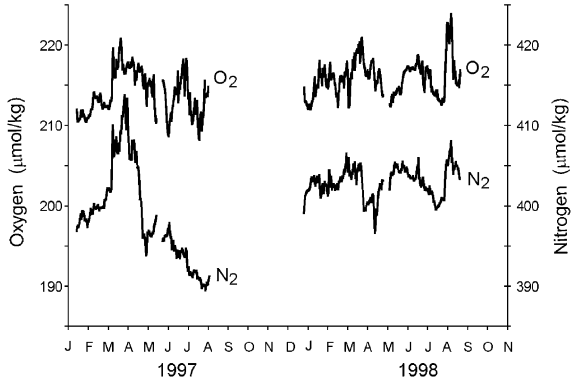


Fig. 7. Daily mean nitrogen gas (lower line) and oxygen concentrations (upper line) as a function of time during the HALE 1–4 deployments. [N_2] was calculated from the GTD–CTD-O_2 data and Eqs. (5b) and (7).

gases to the atmosphere as the temperature at 50 m slowly warmed. The evolution of nitrogen gas concentration in 1998 at this location is much less dramatic, but still episodic with changes of 2–3% on time scales of 1–3 months. The dramatic nitrogen concentration increase of March 1997 coincides with an increase in oxygen concentration (Fig. 7). This oxygen increase must have been produced by net biological oxygen production because the oxygen concentration normally associated with a nitrogen concentration of $415\,\mu mol\,kg^{-1}$ (the value at 50 m in March and normally at about 125 m) is less than that in the mixed layer in winter. The O_2 concentration at 125 m before and after the upwelling event was about $205\,\mu mol\,kg^{-1}$ (Fig. 1). We can make a rough estimate of the net biological O_2 production associated with this event by assuming the increase in O_2 between its "pre-eddy" ambient value ($205\,\mu mol\,kg^{-1}$) and that at 50 m in March ($217\,\mu mol\,kg^{-1}$) occurs over a depth interval of 50 m, which is about the thickness of the oxygen maximum:

$$J_{O_2} = (217 - 205\,\mu mol\,kg^{-1}) \times (1.025\,kg\,l^{-1}) \times (1000\,l\,m^{-3}) \times 50\,m \approx 0.6\,mol\,m^{-2}.$$

This value corresponds to about 40 % of the annual estimated net oxygen production ($1.6\,mol\,m^{-2}\,yr^{-1}$, Emerson et al., 1997).

The other episode of oxygen change in first half of 1997 (Fig. 7) is associated with a gradual decease in the nitrogen gas concentration, indicating that it is not a result of upwelling. If the oxygen concentration were not influenced by biological activity, it would decrease by gas exchange like N_2 concentration. Assuming that the only difference in the geochemistry of N_2 and O_2 is that oxygen is biologically produced, then this oxygen episode (between June and July) requires a biological production of about $0.4\,mol\,O_2\,m^{-2}$ (the concentration change times an assumed depth interval of 50 m). Together these two events, during roughly the first half of the year, account for about 60% of the annual O_2 production of $1.6\,mol\,m^{-2}$. The mechanism causing the net O_2 production in the June–July event is not as clear as that in March, which appears to have responded to nutrient input

from below. Since there is no concomitant decrease in temperature during this period (Fig. 2a) we can rule out the possibility that the increase in O_2 concentration is a result of migration of the sensor between the oxygen maximum (between 50 and 100 m) and the water above. In this case the O_2 production may be in response to nitrogen fixation, since it is known that this mechanism supplies about half of the nitrogen necessary to explain the biological carbon pump in this area (Karl et al., 1997). This calculation demonstrates the utility of the total gas measurement. By determining nitrogen gas concentration from the GTD and O_2 instruments, one knows the effect of mixing, bubbles and gas exchange on the concentration of an inert gas and can use this to distinguish the physical and biological mechanisms causing the oxygen concentration changes.

The oxygen episodes of 1998 coincide approximately with similar changes in nitrogen indicating that they may result from upwelling or eddy events of smaller magnitude than that of March 1997. Only the last one in July August has signatures in the temperature and salinity (Fig. 2) suggesting it results from a large mesoscale eddy that entered the area.

Episodes of oxygen concentration increase produce pulses of O_2 supersaturation (Fig. 8). This is further indication that the episodes are a result of biological production since mixing of water from below, at least before the shallow oxygen maximum forms in July, cannot produce supersaturation since both temperature and oxygen concentration are mixed. The oxygen supersaturation is not always contemporaneous with the oxygen increase. This is indicated dramatically in the event of March 1997. Between March and May of 1997 (Fig. 8) upwelling of water with both higher nitrogen gas concentration and lower temperature resulted in almost no change in the degree of nitrogen supersaturation. Since oxygen poor waters were upwelled, the increase in oxygen due to biological production was just sufficient to bring the oxygen concentration back to saturation while the eddy was in the area (March–mid-April). Only after the event, when the temperature and salinity return to non-eddy values (after mid-April), is there evidence of an oxygen supersaturation signal in excess of the nitrogen supersaturation. This indicates that the processes that produced oxygen supersaturation were no longer associated with the eddy, suggesting that some of the nutrients brought from depth mixed out of the eddy into the surrounding waters of the surface ocean, probably as dissolved organic nitrogen and phosphorus, which has been shown to be associated with eddies in this area (see Emerson et al., 2001 for a further explanation.). It is also clear from this analysis that any attempt to determine the value of net oxygen production from the O_2 supersaturation alone would be misleading. The oxygen concentration-depth profile, and the associated changes in nitrogen gas and temperature, are necessary to accurately determine the net production of oxygen.

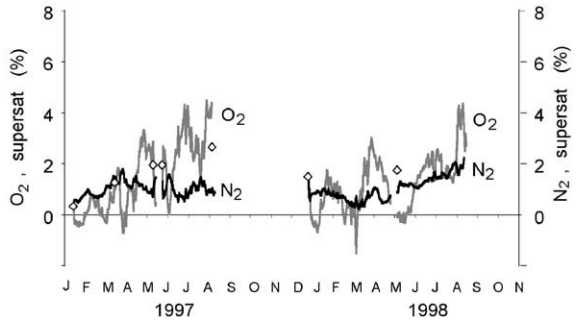


Fig. 8. Daily mean degree of supersaturation for oxygen and nitrogen as a function of time during the HALE 1–4 deployments. The nitrogen supersaturation was calculated from the solubility, total gas pressure (GTD) and pO_2 results. Diamonds are the results of independent measurements of N_2 supersaturation on water samples (Table 1).

5. Conclusions

Nearly two full years of GTD–CTD-O_2 sensor deployment on the deep-sea mooring at the Hawaii Ocean Time series (HOT) have produced results that are readily interpretable in terms of nitrogen and oxygen gas changes caused by mixing, air-water exchange and biological processes. The (GTD) is capable of highly accurate and precise measurements. This is assessed by comparing the degree of nitrogen saturation,

determined from Eqs. (5b), (6) and (7), with independent measurements of nitrogen compiled in Table 1. Seven independent nitrogen gas measurements are on average $0.4 \pm 0.4\%$ greater than the nitrogen supersaturation determined from the in situ data (Fig. 8). Since the data are presented as percent supersaturation, any error in the gas saturation values cancel. As the uncertainty in the individual nitrogen gas measurements is on the order of $\pm 0.2\%$ (Emerson et al., 1999), these results indicate that our in situ determinations are accurate to better than $\pm 0.5\%$.

The oxygen concentration at 50 m at HOT exhibits a series of episodic changes (increases of 2–4% followed by similar decreases) from spring to late summer. These episodes are sometimes associated with similar changes in nitrogen gas, indicating they are the result of shoaling of isopycnals and/or upwelling associated with eddies (Letelier et al., 2000; McGillicuddy and Robinson, 1997). The two most dramatic episodes (May 1997 and August 1998) are associated with large changes in the sea-surface height as determined from TOPEX satellite measurements (Fig. 9). Increases in oxygen and nitrogen at other times may be due to similar mechanisms of smaller scale; however, with only one sensor it is difficult to determine whether the smaller events in late summer represent an increase in the oxygen pressure in the entire euphotic zone or shoaling of the shallow oxygen maximum. Those O_2 episodes not associated with N_2 gas increases or movement of the O_2 maximum indicate mechanisms other than nutrient fluxes from below are stimulating net O_2 production, e.g., near-surface N_2 fixation.

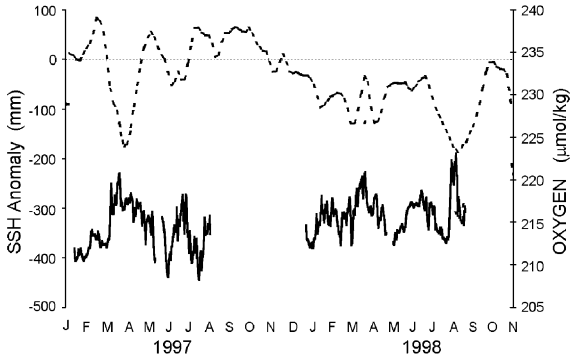


Fig. 9. The sea surface height (SSH) anomaly (mm) determined from TOPEX satellite data in the vicinity of the HALE mooring during 1997 and 1998 (broken line) along with the oxygen concentration (solid line) from Fig. 3. The SSH anomaly data are courtesy of K. S. Johnson (personnel communication) and represent the difference in SSH measurements from the 4-year mean for the period 1993–1996 determined at each 1° grid point. (See the web site http://oceanesip.jpl.nasa.gov/gui/ for more information).

Data from both continuous oxygen and total gas pressure measurements allow separation of the effects of net biological O_2 production and physical processes that change gas concentrations. With the available data it is not possible to determine an accurate value of the net biological oxygen production in the entire euphotic zone, because this quantity depends on depth-integrated changes and fluxes at the air-water and thermocline boundaries. It will require more instruments or a vehicle capable of profiling to derive the depth coverage necessary for this purpose. The most significant error in this approach for measuring the annual oxygen mass balance is caused by drift in the oxygen sensors. Without calibration on a monthly basis the data would be interpretable during only the first few months of deployment. In order for this method to be applicable to the interpretation of net biological oxygen production using remote deployments without frequent calibration, the method of oxygen determination will have to be improved. Either a sensor that is much less prone to drift or a method of in situ calibration must be developed.

Acknowledgements

We would like to thank Terry Houlihan of the HOT program for directing the deployment of the mooring and David Farmer for collaborating in the construction of the GTD–CTD-O_2 instrument. Discussions with Roberta Hamme have been helpful in creating the final version of the manuscript. The sea surface height values from TOPEX satellite data were kindly supplied by Ken Johnson of MBARI. This research was supported by NSF Grants OCE-9906922 (S.E.), and OCE-9601850

and OCE-9617409 (D.K.). This is USJGOFS publication number.

References

Anderson, M.L., Johnson, B.D., 1992. Gas transfer: a gas tension method for studying equilibration across a gas water interface. Journal of Geophysical Research 97, 17899–17904.

Benson, B.B., Krause Jr., D., 1984. The concentration and isotopic fractionation of oxygen dissolved in freshwater and seawater in equilibrium with the atmosphere. Limnology and Oceanography 29, 620–632.

Brandrup, J., Immergut, E. H., Grulke, E.A. (Eds.), Polymer Handbook, Fourth Edition, Wiley, New York, pp. VI-558–559.

Craig, H., Hayward, T.L., 1987. Oxygen supersaturation in the ocean: biological versus physical contributions. Science 235, 199–202.

Emerson, S., Quay, P.D., Stump, C., Wilbur, D., Schudlich, R., 1995. Chemical tracers of productivity and respiration in the subtropical Pacific Ocean. Journal of Geophysical Research 100, 15873–15887.

Emerson, S., Quay, P.D., Karl, D., Winn, C., Tupas, L., Landry, M., 1997. The carbon pump in the Subtropical Pacific Ocean: implications for the global carbon cycle. Nature 389, 951–954.

Emerson, S., Stump, C., Wilbur, D., Quay, P.D., 1999. Accurate measurements of O_2, N_2, and Ar gases in water and the solubility of N_2. Marine Chemistry 64, 337–347.

Emerson, S., Mecking, S., Abell, J., 2001. The biological pump in the subtropical North Pacific Ocean: nutrient sources, redfield ratios and recent changes. Global Biogeochemical Cycles 15, 535–554.

Farmer, D.M., McNeil, C.L., Johnson, .B.D., 1993. Evidence for the importance of bubbles in increasing air-sea gas flux. Nature 361, 620–623.

Garcia, H.E., Gordon, L.I., 1992. Oxygen solubility in seawater: better fitting equations. Limnology and Oceanography 37, 1307–1312.

Glueckauf, E., 1951. The composition of atmospheric air. In: Malone, T.F. (Ed.), Compendium of Meteorology. American Meteorological Society, Boston, pp. 3–10.

Karl, D.M., et al., 1997. The role of nitrogen fixation in biogeochemical cycling in the subtropical North Pacific Ocean. Nature 388, 533–538.

Letelier, R.M., et al., 2000. Role of late winter mesoscale events in the biogeochemical variability of the upper water column of the North Pacific Subtropical Gyre. Journal of Geophysical Research 105, 28723–28739.

McGillicuddy, D.J., Robinson, A.R., 1997. Eddy induced nutrient supply and new production in the Sargasso Sea. Deep-Sea Research I 44, 1427–1449.

McNeil, C.L., Johnson, B.D., Farmer, D.M., 1995. In situ measurements of dissolved nitrogen and oxygen in the ocean. Deep-Sea Research I 42, 819–826.

Spitzer, W.S., Jenkins, W.J., 1989. Rates of vertical mixing, gas exchange and new production: estimates from seasonal gas cycles in the upper ocean near Bermuda. Journal of Marine Research 47, 169–196.

Takahashi, T.T., et al., 1997. Global air-sea flux of CO2: an estimate based on measurements of the sea-air p_{CO_2} difference. Proceedings of the National Academy of Science USA 94, 8292–8299.

Weiss, R.F., 1970. The solubility of nitrogen, oxygen and argon in water and seawater. Deep-Sea Research 17, 721–735.